Relevancy of Pulsed Electroacoustic Measurements for Investigating Spacecraft Charging

Zachary Gibson, *Member, IEEE,* and J. R. Dennison, *Member, IEEE*

***Abstract*—The magnitude and spatial distribution of charge embedded in dielectric materials and the evolution of the charge distributions with time are paramount for the understanding and mitigation of spacecraft charging. Spacecraft materials are charged primarily by incident fluxes of low energy electrons, with electron fluxes in the 10 keV to 50 keV range often responsible for the most deleterious arcing effects. While the pulsed electroacoustic (PEA) method can provide sensitive non-destructive measurements of the internal charge distribution in insulating materials, it has often been limited for spacecraft charging applications by typical spatial resolutions of ≤10 µm, with a 10 µm range of electrons in common spacecraft materials (e.g., PEEK, PTFE, LDPE or SiO_2) at incident energies from ~20 keV to ~40 keV. A series of PEA tests over a range of incident electron energies were devised to investigate the relevance of the PEA method for typical spacecraft charging applications. Thin film samples of vacuum baked polyether-etherketone (PEEK) were irradiated with 10 keV to 80 keV mono-energetic electron beams. PEA measurements of deposited charge profiles determined the peak positions and magnitude of deposited charge. These were used to establish the minimum incident energies for which PEA measurements provided meaningful results and thus to characterize the merits of PEA measurements over energy ranges of relevancy to spacecraft charging issues.**

***Index Terms*—spacecraft charging, irradiation, polymers, pulsed electroacoustic method, space charge**

I. INTRODUCTION

To assure successful space missions, spacecraft charging must be understood and mitigated. The most important factor for dielectric spacecraft materials is arguably the internal electric field, which is determined by the internal charge distribution. There are many ways to attempt to determine what the electric field is inside a material. Measurements of material properties can help to inform through analytical formulas [1] or simulations such as *AF-NUMIT3* [2], *JPL NUMIT* [3], and *DICTAT* [4]. Necessary parameters for these calculations can include material properties that can be experimentally determined [5] such as the bulk conductivity/resistivity [6], breakdown field strength [7], radiation induced conductivity [8, 9], delayed radiation induced conductivity [10], photoyield, electron yield, ion yield, and permittivity [11]. However, these measurements are indirect and only help to provide inferred values of the internal field when materials are exposed to the space environment. The most direct way to measure the details of the internal electric field is to determine the distribution and magnitude of the embedded charge. This is precisely the information non-destructive, dynamic pulsed electroacoustic measurements can directly provide. Direct knowledge of the magnitude and spatial distribution of embedded charge from PEA allows direct calculation of the internal electric fields, which drive charge transport and electrostatic breakdown. Other measurement methods, such as surface potential or electrostatic discharge measurements, rather provide averaged or integrated information about charge distributions. This is particularly evident in samples having undergone electrostatic breakdown [12]. While measurements of conductivity and radiation induced conductivity can provide estimations of charge dynamics, direct measurement of embedded charge distributions over time allow observation of the actual charge dynamics as well as validation for simulations of deep dielectric charging and charge transport. [13].

The pulsed electroacoustic (PEA) method provides nondestructive measurements of charge distributions in dielectric materials [14-16]. Charge can be deposited into a material through high voltage DC bias or via irradiation with a beam of charged particles in the lab. Open PEA (or non-contact) systems can deposit charge via irradiation with no electrode on the front surface of the sample [17, 18] and short circuit or ambient PEA systems have electrodes on the front surface [14] (both have rear electrodes). There can be substantial differences in the results depending on the electrode configuration [19, 20]. Only 1D parallel plate capacitor and 1D radial cylindrical cable geometries [21-25] are typically measured using the PEA method [26, 27], though lateral charge distributions and even 3D charge distributions can be measured with systems with multiple sensor arrays [28-30]. Given the micron scale penetration depths most applicable for spacecraft charging applications and typical micron thicknesses of thin thermal blankets, solar coverglasses, or thermal paints as compared to centimeter diameters of typical PEA electrodes, 1D measurements are reasonable approximations [15].

This is the accepted version of the paper with the full version being available on IEEE Xplore.

This work was partially supported by Small Business Technology Transfer Research (STTR) Phase I and Phase II funding from the Air Force Research Laboratory, Kirtland Air Force Base, Albuquerque, New Mexico, USA. Gibson acknowledges support through a Presidential Doctoral Research Fellowship from the Utah State University Office of Research. *(Corresponding author: Z. Gibson).*

Zachary Gibson is with Utah State University, Logan, UT 84322 USA (e-mail: zack.gibson@usu.edu)

J.R. Dennison is with Utah State University, Logan, UT 84322 USA (e-mail: jr.dennison@usu.edu)

Color versions of one or more of the figures in this article are available online at http://ieeexplore.ieee.org

Z. Gibson and J. R. Dennison, "Relevancy of Pulsed Electroacoustic Measurements for Investigating Spacecraft Charging," in IEEE Transactions on Plasma Science, doi: 10.1109/TPS.2023.3244058.

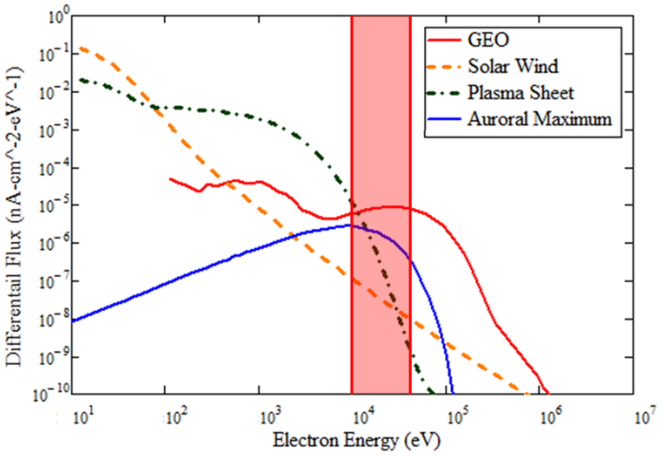

Fig. 1. Representative space electron environment fluxes versus electron energy. Modified from [33] and based on values from Minow. Red shaded region is the incident electron energy range identified as a critical to charging.

The actual internal electric fields can then be calculated from the measured charge distributions. The PEA system appears to be an excellent tool for quantifying and understanding spacecraft charging. This study aims to test the relevancy of PEA measurements in the context of spacecraft charging. In particular, it addresses the question of what are the lowest incident energy electrons that can produce charge distribution peaks that are resolvable with a typical PEA system as a criterion for the utility of PEA measurements for the incident electron energies most commonly encountered in spacecraft charging events. This was done by irradiating a typical spacecraft material, polyether-etherketone (PEEK), with an electron beam with energies in the energy regime typical for spacecraft charging. PEEK was chosen as the test material since its very low conductivity meant that deposited charge can be considered stationary for the timescale of the PEA experiments [6]. The relatively low acoustic attenuation and dispersion of PEEK allows for more accurate PEA measurements of the internal charge distribution [13]. Though PEEK is an optimal material to measure with the PEA system, the proposed study is feasible with other common polymeric, glass, and ceramic spacecraft materials which have been studied with PEA methods.

An overview of typical representative space environments and spacecraft charging conditions and incident electron energies, as well as the relevant length scales, are presented. The experimental details are then outlined and the PEA results presented. The paper ends with a discussion of the relevance of these results to spacecraft charging applications and conclusions from the study.

II. Space Environment

This section outlines representative electron space environments and typical spacecraft charging conditions. It concludes with identifying the relevant length scales in the regime of incident electron energies most relevant to spacecraft charging. The focus is on the electron environment, as electrons drive most of the charging in the space environment [31, 32].

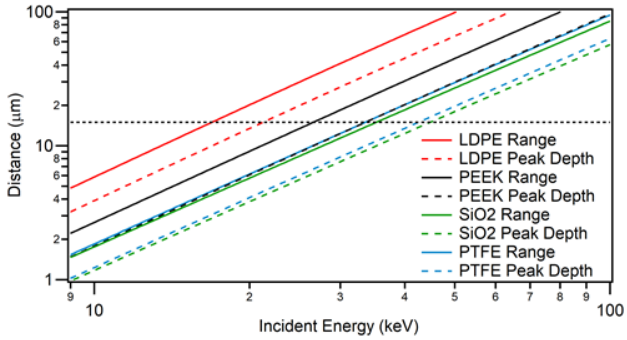

Fig. 2. The electron range for several representative spacecraft materials as a function of energy, produced with MPG Electron Range Approximation Tool v1.1 [41-43]. Dashed lines indicate peak deposition depths as estimated by 2/3 of the range. The dashed black line is a distance of 15 µm, indicating when the most accurate results are obtained with a 10 µm resolution PEA system.

A. Typical Near-Earth Orbit Electron Environments

Fig. 1 presents typical differential electron fluxes in near-Earth orbits, as well for lunar and interplanetary environments, as a function of electron energy [33]. Plotting differential fluxes as a function of electron energy are useful as the area under the curve corresponds to the total number of electrons in the energy range of interest. Space environments typically have higher flux at lower energies.

B. Typical Spacecraft Charging Conditions

Reference [34] suggests there appears to be a threshold electron energy for charging of a spacecraft to occur. Data from ATS6 and SCATHA missions showing the spacecraft potential as a function of electron energy are plotted in Fig. 3 of Ref. [34]. There is an onset or cut-off energy around 10 keV where charging appears to begin. Reference [34] discusses a "critical charging regime" for spacecraft that can vary from 10 keV to 80 keV: "...it appears that the spacecraft does not charge unless there are substantial (electron) fluxes between 10 and 20 keV." Other literature offers similar conclusions [35-38]. This indicates that the electron energies of particular importance for spacecraft charging are in the region of 10 keV to 50 keV (highlighted in red in Fig. 1), and perhaps up to 80 keV or more.

The magnitude of the discharge is also important for spacecraft charging anomalies, which understandably depends on the magnitude of the charge present. Reference [5] estimates the magnitude of electrostatic discharge severity for minor events is up to 500 nC, moderate events is up to 2 µC, and severe events is up to 10 µC.

The incident electron energy range of 10 keV to 50 keV is identified as a critical energy range from these observations for spacecraft charging. This range of incident energies needs to be correlated to a length scale to be measured with PEA to address the relevance of PEA measurements to spacecraft charging studies.

Z. Gibson and J. R. Dennison, "Relevancy of Pulsed Electroacoustic Measurements for Investigating Spacecraft Charging," in IEEE Transactions on Plasma Science, doi: 10.1109/TPS.2023.3244058.

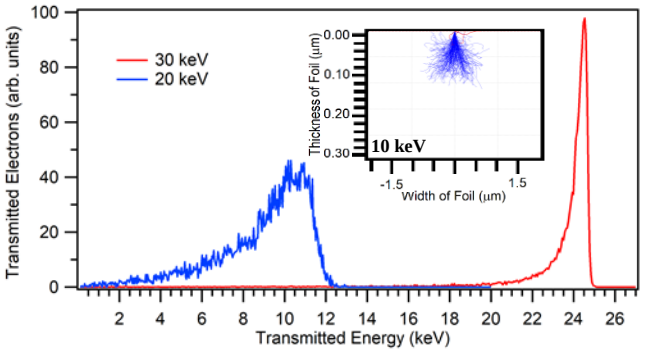

Fig. 3. Transmitted electron energies through C foil as simulated with CASINO v2.51 [47] for 20 keV and 30 keV incident electrons. Inset depicts CASINO electron trajectory simulation of 10 keV incident electrons within the C foil.

C. Length Scales for Spacecraft Charging

It is helpful to consider two parameters to map the electron energy regime of interest into relevant length scales. These are the peak deposition depth and range of the incident electrons. The peak deposition depth is the depth at which the maximum amount of charge is deposited. This can be seen in PEA measurements as the peak of the measured charge distribution (blue dashed line in Fig. 4). The range is the maximum depth even a single electron reaches into the material at a given incident electron energy. The peak deposition depth has been estimated as 2/3 of the range [39]. The range for numerous materials at energies ≥10 keV have been modeled and tabulated; refer to ESTAR at NIST [40]. The Material Physics Group (MPG) Electron Range Approximation Tool used here is in excellent agreement for the materials tabulated in ESTAR [41]. The MPG tool provides the ability to predict the electron range for arbitrary materials down to lower energies ≲10 eV using only the stoichiometry, density, and bandgap [42, 43]. This capability was exploited to predict the range in PEEK.

The range for four ubiquitous insulating spacecraft materials, low density polyethylene (LDPE), polytetrafluoroethylene (PTFE), silicon glass (SiO_2) and polyether-etherketone (PEEK), are plotted over the relevant energy range for spacecraft charging in Fig. 2. Range depends on a number of factors, but largely on the mean atomic number, Z, of a material. LDPE and PTFE span the range from low Z to high Z, respectively (and hence low to high ranges at a given energy) for common spacecraft polymeric insulators. Silicon glass is a common spacecraft dielectric with higher Z and lower range. The focus of this study is PEEK with intermediate range values and advantageous acoustic properties for PEA measurements.

III. Experiment

Table I lists the details for electron beam irradiation of PEEK samples irradiated with nominal incident electron energies of 10 keV, 20 keV, and 30 keV presented in this study. It also includes representative measurements from a previous study for PEEK samples irradiated with 50 keV and 80 keV electrons. Sample and irradiation details for samples irradiated with 50 keV and 80 keV incident electron energies can be found in [13].

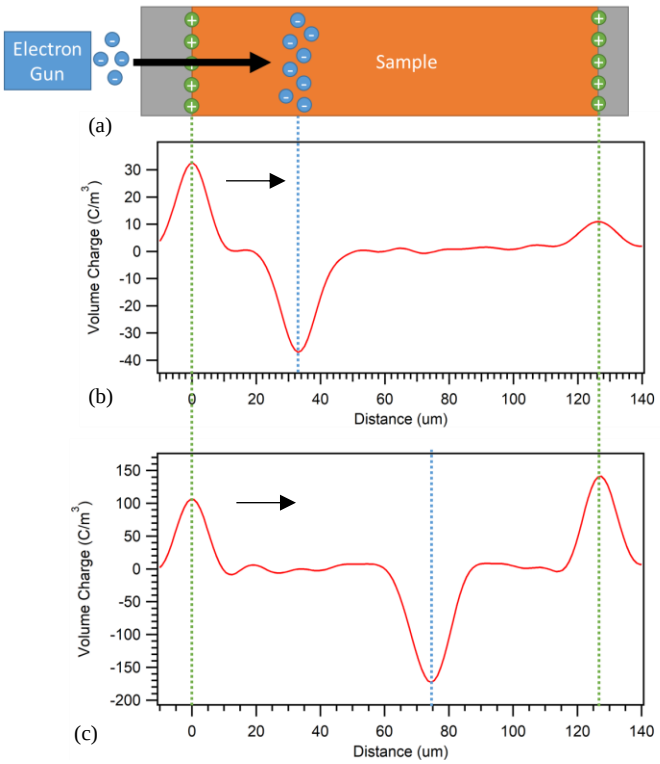

Fig. 4. Results for PEEK irradiated with electrons are plotted along with (a) representative images for the PEA sample stack. Note that the samples are irradiated without a front electrode present. The black arrows indicates the direction of the incident electron beam. Results are shown for (b) 50 keV and (c) 80 keV incident electrons. The green dashed lines indicate the interfacial charge distributions and the blue dashed lines indicate the peak of the deposited charge distributions.

A. Sample Details

The samples of PEEK used in this experiment are from APTIV Victrex PEEK Film Technology and are nominally 125 μm thick (PN 1000-125G) [44]. The thickness of the samples were measured with a micrometer (Mitutoyo IP65; ±0.5 μm resolution). These thicknesses were used in the calibration of the PEA depth measurements [45]. The samples were cut into discs of 3.4 cm diameter and baked out at 100°C for ≥72 hrs under $<10^{-4}$ hPa vacuum to minimize water and other volatile compound content. As the optical bandgap of PEEK is ~3.1 eV [46], the samples were not exposed to ambient light (to only red light) to avoid any potential photo-charging/discharging at all times after bake out. A total of six samples were prepared and irradiated.

B. Irradiation Details

The samples were irradiated with ~65±20 pA/cm^2 for a total of 4 minutes each. A pair of samples were irradiated at each incident electron gun energy of 10 keV, 20 keV, and 30 keV, using an 80 keV electron gun (Staib EH-80) at a vacuum level of $\leq 10^{-6}$ hPa at room temperature.

TABLE I
DETAILS OF ELECTRON IRRADIATION AND CHARGE DEPOSITION IN PEEK

Nominal Energy (keV)	*Reduced Energy (keV)*	*Nominal Range (μm)*	*Reduced Range (μm)*	*Nominal Estimated Peak Deposition Depth (μm)*	*Reduced Estimated Peak Deposition Depth (μm)*	*Measured Peak Deposition Depth (μm)***
10	*0**	*2*	*0**	*1*	*0**	*12.5/12.5*
20	*9*	*9*	*2*	*6*	*1*	*11.2/11.6*
30	*24*	*20*	*13*	*13*	*9*	*10.1/10.6*
50	*-*	*45*	*-*	*30*	*-*	*32.9*
80	*-*	*100*	*-*	*67*	*-*	*74.4*

'Nominal' indicates the electron energy output by the electron gun and 'reduced' indicates the electron energy as reduced by passing through the C foil.
*CASINO simulation [47] indicated electrons would not penetrate the C scattering foil so incident energy is unknown but ≲10keV (refer to Fig. 3 inset).
**A pair of values is given for each pair of PEEK samples irradiated under the same conditions.

A single layer of 595 μg/cm^2 graphitic carbon scattering foil (ACF – Metals) was used to produce a broad uniform (approximately Gaussian) electron beam (~6.4 cm full width at half maximum [FWHM]) with an approximate beam intensity variation of ±25% over each 3.4 cm diameter sample area. The beam profile incident on the samples was measured with a Faraday cup. The scattering foil resulted in reduced and broadened energy distributions, particularly at the lower nominal incident energies. Table I lists both the nominal and reduced values for incident electron energy, range, and peak deposition depth. The reduced energy distribution was modeled with CASINO v2.51 [47] and the average transmitted energies are shown as the reduced energy of Table I. Note that the 50 keV and 80 keV irradiations were done in a different facility with no C foil correction necessary [13]. The CASINO simulations indicated that the electrons should not have penetrated the C foil at 10 keV (refer to Fig. 3 inset), but charge was measured deposited in the sample (refer to Fig. 5). The resulting electron energy distributions are skewed to lower energies with a FWHM for 20 keV and 30 keV nominal incident energy of ~2.4 μm and ~0.6 μm, respectively (refer to Fig. 3).

After irradiation, the samples were removed from vacuum, stored in an Ar purged container and transported to be measured with the PEA system elsewhere in the lab. Note that the PEA measurements were obtained in ambient conditions.

C. Pulsed Electroacoustic Method

The PEA method works in a parallel plate capacitor configuration [14, 15]. The sample is clamped between two electrodes and a voltage is pulsed across the sample. This applies a coulombic force to embedded charge in the sample, resulting in an acoustic pressure wave. This acoustic pressure wave propagates through the sample and to the back of the rear electrode where it is measured with a piezoelectric sensor. The signal from the piezoelectric sensor is measured by an oscilloscope. Simple time of flight in conjunction with the material speed of sound allows for measurements in time to be converted to distance. The speed of sound is determined by dividing the measured sample thickness by the time difference between the two interfacial peaks [45]. The PEA system response function is then removed through deconvolution and the amplitude is then calibrated as a charge density with a reference measurement where a small DC bias is applied [13, 48].

In the Utah State University (USU) PEA system, and typical PEA systems, the spatial resolution is ~10 μm [13, 15]. The spatial resolution of PEA measurements are typically defined as the FWHM of the leading interfacial peak [49, 50]. The spatial resolution of the USU PEA system for measurements of PEEK have been determined to be 10.6±1.1 μm [13]. Note that the spatial resolution is determined by several factors, including the speed of sound which is material dependent. The uncertainty in the peak deposition depth is ≤0.5 μm [13, 45].

IV. RESULTS

Measurements of the irradiated samples were obtained in two orientations relative to the embedding beam direction, by flipping the samples over, such that the apparent direction of incident electrons are from the left or from the right. Only the measurements with left incidence are presented as they are much easier to align and compare as opposed to the right incidence measurements, which is particularly important for the 10 keV, 20 keV, and 30 keV incident energies. It should be noted that in this orientation there are also less attenuation and dispersion effects for the measured charge distribution, though this is not an issue for PEEK.

Fig. 4 shows charge profiles for PEEK samples irradiated with 50 keV and 80 keV electrons. Fig. 4 indicates the location of the interfacial and deposited charge in the measurements, referenced to the sample and PEA system. Note that the electrode on the irradiated surface of the sample is not present during irradiation. In this case, the electrons are incident from the left, as indicated by the arrows. The embedded negative charge distribution produces a positive mirror charge on the surface of the front and rear electrodes, as seen at the interfaces and indicated with the green dashed lines. The width of the leading interfacial peak (the left peak) is a measure of the spatial resolution of the system [49, 50]. This feature should be the response of the PEA system to essentially a delta function of charge on the surface of that electrode.

Z. Gibson and J. R. Dennison, "Relevancy of Pulsed Electroacoustic Measurements for Investigating Spacecraft Charging," in IEEE Transactions on Plasma Science, doi: 10.1109/TPS.2023.3244058.

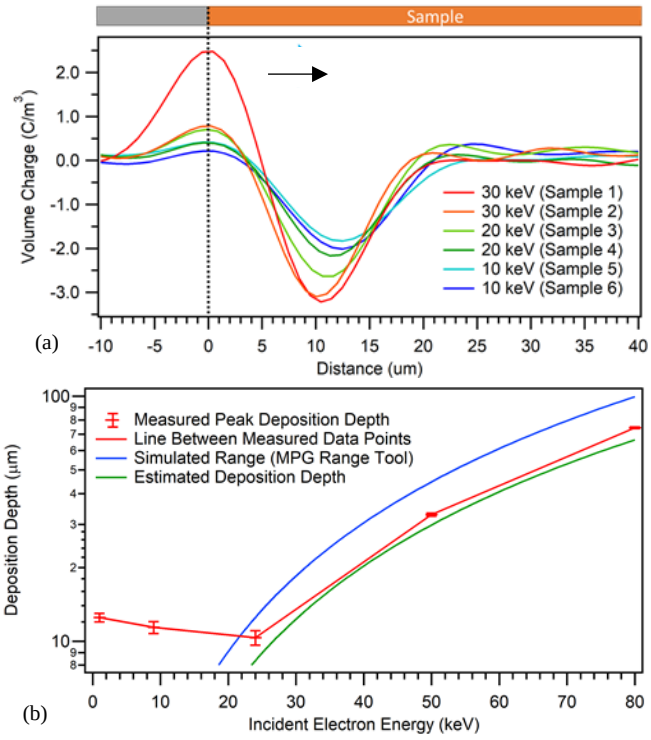

Fig. 5. (a) PEA measurements of PEEK irradiated with 10 keV, 20 keV, and 30 keV electrons are plotted. Only the section of the data near the irradiated surface is shown as the charge is deposited at shallow depths. (b) The measured peak deposition depth versus incident electron energy is plotted with the range determined from the MPG Electron Range Approximation Tool v1.1 [41-43] and the deposition depth estimated as 2/3 of the range.

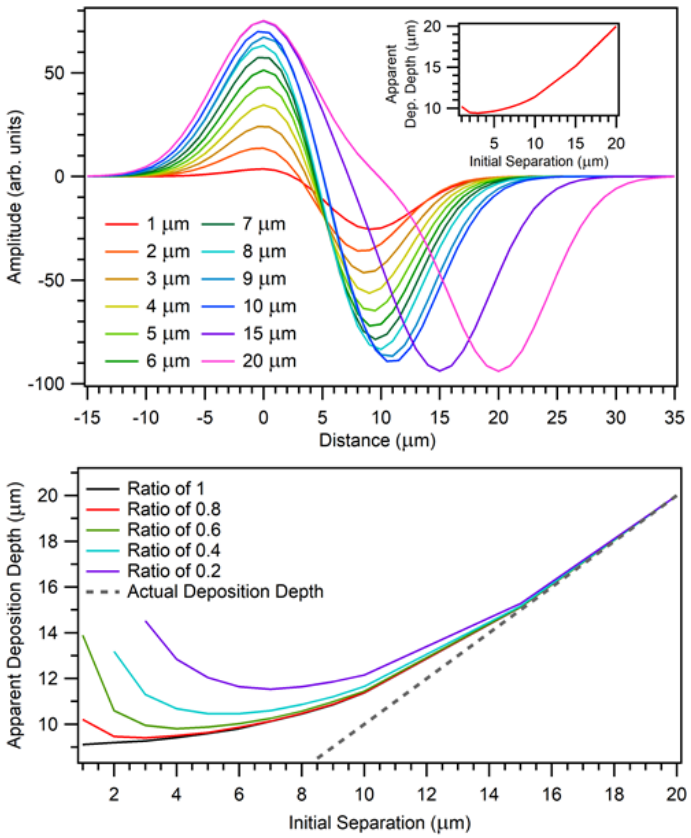

Fig. 6. (a) Superposition of two Gaussian distributions, one positive and one negative, with varying separations of the maxima. The positive distribution is scaled to 0.8 the amplitude of the negative distribution. The inset shows the resulting apparent deposition depth (peak-to-peak distance from positive to negative peak). (b) Plotted is a family of curves with various ratios of the amplitude of the positive distribution, including the plotted inset of (a).

Referring to Fig. 4, the PEEK sample irradiated with 80 keV electrons has a charge distribution with a peak deposition depth of 74.4±0.5 μm [13] and the sample irradiated with 50 keV electrons has a peak deposition depth of 32.9±0.3 μm [13, 45]. The peak deposition depth here is the peak-to-peak distance of the irradiated surface's interfacial peak to the embedded charge peak, *e.g.* from the left green dashed line to the blue dashed line in Fig. 4(b) and Fig. 4(c). The results for the nominal incident electron energies of 10 keV, 20 keV, and 30 keV can be seen in Fig. 5. The measured peak deposition depths are presented in Table I and the average values are plotted in Fig. 5(b). The pairs of measurements for each incident energy differ by ≤0.5 μm, which is on the order of the uncertainty and small compared to the apparent shifts of deposition depth between incident energies of ~1 μm for 10 keV, 20 keV, and 30 keV incident energies. This suggests that these shifts are real and not just a result of the variations due to instrument or sample effects.

There is a counterintuitive trend apparent in Fig. 5(b) for the measured peak deposition depth to *decrease* with *increasing* incident energy below ~25 keV. Possible causes for this phenomena include new physics (unlikely), effects of deconvolution, and mischaracterization of deposition depth due to superimposed charge distributions. To study the latter possible cause of this phenomena, a simple model was devised which can offer a qualitative explanation of this observation. This is a simple model of a negative embedded charge distribution near the surface in superposition with a positive interfacial charge distribution.

V. A Simple Model

Consider two Gaussian peaks, one positive and one negative, which are added together with varying peak-to-peak separations. If the Gaussians are of equal magnitude then the intuitively expected trend is observed; that is, the larger the separation between the initial Gaussian peaks, the larger the modeled separation in the peak-to-peak distance of the superimposed distributions, depicted as ratio of 1 in Fig. 6(b). However, this does not agree with the observed PEA measurements.

This model with equal magnitude peaks is not representative for the PEA measurements. There is a lower magnitude charge distribution at the incident interface, due to the exciting pulse of the PEA system and a small amount of mirror charge at the opposite electrode. The pulse has an effect on the measured interfacial charge distribution [48], particularly when there is only a small amount of charge being

measured in the bulk, as is the case for the PEA measurements in this study.

When the first positive Gaussian is reduced in magnitude as compared to the negative distribution, then a different trend emerges. As the separation between the initial Gaussians is increased, there is a trend in the resulting distribution of decreasing peak-to-peak distance with increasing initial separations (at small initial separations), followed by a return to the trend for increasing peak-to-peak distance with increasing peak separations modeled for equal peak amplitudes. This is illustrated in Fig. 6(a), which uses Gaussians of 10 μm FWHM with separations of 1 μm to 20 μm with the positive interfacial distribution having 0.8 times less magnitude than the negative distribution. At low initial separations, there is a small decrease in the resulting peak-to-peak distances before this then increases again; refer to inset of Fig. 6(a).

Fig. 6(b) reproduces this inset, along with a family of such curves with ratios of interfacial positive peak magnitude to embedded charge negative peak amplitude at 1.0, 0.8, 0.6, 0.4, and 0.2. The results show that the apparent deposition depth increases with decreasing initial separation when the initial separation is low enough. This effect is enhanced with a larger difference in the initial magnitude of superimposed Gaussians (ratio further from 1). The dashed line indicates the actual deposition depth (which is the initial peak-to-peak distance between the two Gaussians). At approximately ~1.5x the spatial resolution (FWHM of the Gaussians), the difference between the apparent deposition depth and the actual deposition depth become essentially negligible. This suggests that the most accurate PEA results can be obtained for measurements where the charge distributions are separated by at least 1.5x the spatial resolution.

VI. Discussion

The PEEK samples irradiated with 80 keV and 50 keV electrons resulted in embedded charge distributions that are easily measured with the PEA system [13]. This clearly demonstrates the applicability of PEA measurements in the higher energy regime of energies of most interest for spacecraft charging. However, as the samples are irradiated with even lower energy electrons from 30 keV down to 10 keV, the limits of the PEA system become more apparent.

The measurement of a peak deposition depth of 10.4±0.5 μm for the 30 keV irradiated PEEK sample may well be an accurate depiction of the internal charge distribution in the sample. However, this is close to the spatial resolution of the system, which is 10.6±1.1 μm for PEEK [13] (FWHM of leading interfacial peak). The apparent peak deposition depths of 11 μm and 12 μm, for the nominal incident energies of 10 keV and 20 keV respectively, are also comparable to the instrumental FWHM. As the incident electron energy is lowered to nominal energies of 20 keV and 10 keV, there is a very small ($\lesssim$2 μm) apparent shift of the charge distribution deeper into the material evident in Fig. 5. This is non-physical, as charge is expected to be deposited less deep into the material with decreasing energy. This trend is likely due, at least in part, to the effects modeled in Fig. 6. That is, this is due to the superposition of the signal from the interfacial positive peak with the signal from the deposited negative peak in the PEA measurements.

This work indicates that the most accurate results can be obtained when charge distributions are separated by ~1.5x the spatial resolution, as determined by the FWHM of the leading interfacial peak. For the current USU system, and other similar PEA systems, this is on the order of ~15 um, which corresponds to the electron peak deposition depth estimated for a ~30 keV electron beam incident on PEEK and from approximately 20 keV to 45 keV for low to high Z materials, respectively, shown in Fig. 2. A dashed line at 15 μm is plotted to indicate the region of materials and energies where a typical PEA system is likely to have accurate results. However, this is complicated due other factors. The spatial resolution can differ due to the speed of sound of the material measured. Materials with higher conductivity, such as LDPE, may not be easily measured in the same manner of this study as the charge may migrate or dissipate during transport of the sample out of the irradiation chamber to the ambient PEA system or during measurement in the PEA system.

VII. Conclusions

This study has shown the relevancy of PEA measurements for measuring deposited charge distributions in the range of incident electron energies of importance for spacecraft charging. Charge distributions are easily resolved in PEEK for incident energies $\gtrsim$30 keV with the current USU PEA system. Materials with lower Z should be able to be measured in this method with a typical PEA system when irradiated with energies $\gtrsim$20 keV, as long as the conductivity is sufficiently low enough to keep the charge stationary on the timescale of the measurement.

The spatial resolution of the PEA method can be improved, through both experimental enhancements and data processing techniques, to push the resolution of the system to energies $\lesssim$20 keV. It should be noted that at least one PEA system does have spatial resolution on the order of a few microns [51, 52]. PEA systems with this high spatial resolution should be capable of measuring deposited charge distributions from incident electron energies $\lesssim$10 keV, refer to Fig. 2.

Further work is needed to investigate what useful information can be extracted about embedded charge distributions near the surface given that the distributions are on the order of or narrower than the spatial resolution of the measurement. There are also issues with only considering the peak of the charge distributions. Consideration of the rising edge may give a more accurate depiction of deposition depths, but this would not provide any information about the shape of the distribution. Further work should be done to study the other moments of the measured charge distributions to see what useful information can be extracted.

Nominal incident electron energies should be investigated in the range of 15 keV to 50 keV at smaller energy increments to better delineate the range of energies the current PEA system can accurately investigate and to increase confidence in the PEA measurements in this energy range, looking for the charge to be deposited deeper into the sample with increasing energy. The simple model of superimposed Gaussians could be improved to provide quantitative insight and should be explored

Z. Gibson and J. R. Dennison, "Relevancy of Pulsed Electroacoustic Measurements for Investigating Spacecraft Charging," in IEEE Transactions on Plasma Science, doi: 10.1109/TPS.2023.3244058.

further. The convolution of the PEA response function and an expected charge distribution as compared to a raw PEA signal could also provide further insight and intuition.

It is also possible to measure embedded charge distributions near the surface in open electrode configuration PEA systems (often called “open PEA” or “non-contact”) as the excitation electrode is not in physical contact with the sample and therefore there is no measured mirror charge superimposed with the embedded charge signal [17, 18, 53, 54]. This would also allow for higher conductivity materials to be easily measured without worry of charge migration during sample transport as is needed with an ambient PEA system. However, the difficulty then becomes determining the position of the surface of the sample to obtain low absolute error in the distance calibration. This would also provide a poor measurement for materials such as PTFE with high dispersion and attenuation if the sample is too thick. Other methods should be explored such as signal processing to remove the effect of the interfacial charge in ambient PEA measurements. This work is currently in progress [55].

Studies to investigate signal processing and data analysis techniques to improve uncertainties in key parameters of the measured charge distributions, such as the peak of the charge distribution, are already underway [45]. The ability to resolve peak positions to ~1 μm (see Fig. 5 and Ref. [45]) already suggest that such alternative measures of instrumental resolution may extend the validity of PEA measurements to lower energies relevant to spacecraft charging applications. Overall, PEA measurements are a promising tool to aid in the understanding and mitigation of spacecraft charging.

ACKNOWLEDGMENTS

L. H. Pearson, E. W. Griffiths and A. C. Pearson of Box Elder Innovations, LLC were instrumental in the development of the pulsed electroacoustic test system used for the PEA measurements.

REFERENCES

[1] S. B. Rao, "A simple formula for the transmission and absorption of monoenergetic electrons," *Nuclear Instruments and Methods*, vol. 44, pp. 155-156, 1966.

[2] B. P. Beecken, J. T. Englund, J. J. Lake, and B. M. Wallin, "Application of AF-NUMIT2 to the modeling of deep-dielectric spacecraft charging in the space environment," *IEEE Transactions on Plasma Science*, vol. 43, pp. 2817-2827, 2015.

[3] I. Jun, H. B. Garrett, W. Kim, and J. I. Minow, "Review of an Internal Charging Code, NUMIT," *IEEE Transactions on Plasma Science*, vol. 36, pp. 2467-2472, 2008.

[4] D. Rodgers, K. Ryden, G. Wrenn, P. Latham, J. Sorensen, and L. Levy, "An engineering tool for the prediction of internal dielectric charging," in *6th Spacecraft Charging Technology Conference, Hanscom*, 1998.

[5] "Mitigating In-Space Charging Effects - A Guideline," NASA Technical Handbook, NASA-HDBK-4002B, 2022.

[6] B. Wood, D. King, and J. R. Dennison, "Time-Evolved Constant Voltage Conductivity Measurements of Common Spaceborne Polymeric Materials," in *15th Spacecraft Charging Technology Conference*, Kobe University, Kobe, Japan, 2018.

[7] A. Andersen, "The Role of Recoverable and Non-Recoverable Defects in DC Electrical Aging of Highly Disordered Insulating Materials," PhD, Physics, Utah State University, 2018.

[8] J. C. Gillespie, "Temperature Dependence of Radiation Induced Conductivity," PhD, Physics, Utah State University, 2022.

[9] J. Boman, B. Wood, J. Lee, and J. R. Dennison, "New System for Temperature Dependent Radiation Induced Conductivity Measurements," in *Applied Space Environments Conference 2021*, 2021.

[10] G. Yang and G. Sessler, "Radiation-induced conductivity in electron-beam irradiated insulating polymer films," *IEEE transactions on electrical insulation*, vol. 27, pp. 843-848, 1992.

[11] J. Lee, H. Allen, and J. R. Dennison, "Real and Imaginary Permittivity Testing in High-Vacuum and Variable Temperature Settings," in *Applied Space Environments Conference 2021*, Jet Propulsion Laboratory, Pasadena, CA, 2021.

[12] M.-P. Cals, J.-P. Marque, and C. Alquie, "Direct observation of space charge evolution in e-irradiated Kapton films," *IEEE transactions on electrical insulation*, vol. 27, pp. 763-767, 1992.

[13] Z. Gibson, J. R. Dennison, B. Beecken, and R. Hoffman, "Comparison of Pulsed Electroacoustic Measurements and AF-NUMIT3 Modeling of Polymers Irradiated with Monoenergetic Electrons," *Journal of Spacecraft and Rockets*, (To be published).

[14] T. Maeno, T. Futami, H. Kushibe, T. Takada, and C. Cooke, "Measurement of spatial charge distribution in thick dielectrics using the pulsed electroacoustic method," *IEEE transactions on Electrical Insulation*, vol. 23, pp. 433-439, 1988.

[15] J. R. Dennison and L. H. Pearson, "Pulsed electro-acoustic (PEA) measurements of embedded charge distributions," in *Nanophotonics and Macrophotonics for Space Environments VII*, 2013, p. 887612.

[16] V. Griseri, "Pulsed Electroacoustic Method," in *Dielectric Materials for Electrical Engineering*, ed, 2010, pp. 229-250.

[17] J. Riffaud, V. Griseri, and L. Berquez, "New design of the pulsed electro-acoustic upper electrode for space charge measurements during electronic irradiation," *Rev Sci Instrum*, vol. 87, p. 073901, Jul 2016.

[18] V. Griseri, K. Fukunaga, T. Maeno, C. Laurent, D. Payan, and L. Levy, "Assessment of measuring conditions with the pulse electro-acoustic system adapted to work under electronic irradiation," in *Electrical Insulation and Dielectric Phenomena, 2003. Annual Report. Conference on*, 2003, pp. 20-23.

[19] C. Perrin, V. Griseri, and C. Laurent, "Measurement of internal charge distribution in dielectrics using the pulsed electro-acoustic method in non contact mode," *IEEE Transactions on Dielectrics and Electrical Insulation*, vol. 15, pp. 958-964, 2008.

[20] A. Andersen, K. Wousik, J. R. Dennison, B. Wood, T. Schneider, J. Vaughn, *et al.*, "Spacecraft Charging Test Considerations for Composite Materials," presented at the 16th Spacecraft Charging Technology Conference, Virtual, 2022.

[21] M. Fu, G. Chen, A. Davies, Y. Tanaka, and T. Takada, "A modified PEA space charge measuring system for power cables," in *Proceedings of the 6th International Conference on Properties and Applications of Dielectric Materials (Cat. No. 00CH36347)*, 2000, pp. 104-107.

[22] K. Fukunaga, H. Miyata, M. Sugimori, and T. Takada, "Measurement of charge distribution in the insulation of cables using pulsed electroacoustic method," *IEEJ Transactions on Fundamentals and Materials*, vol. 110, pp. 647-648, 1990.

[23] M. Fu and G. Chen, "Space charge measurement in polymer insulated power cables using flat ground electrode PEA system," *IEE Proceedings-Science, Measurement and Technology*, vol. 150, pp. 89-96, 2003.

[24] N. Hozumi, H. Suzuki, T. Okamoto, K. Watanabe, and A. Watanabe, "Direct observation of time-dependent space charge profiles in XLPE cable under high electric fields," *IEEE Transactions on Dielectrics and Electrical Insulation*, vol. 1, pp. 1068-1076, 1994.

[25] N. Hozumi, T. Takeda, H. Suzuki, and T. Okamoto, "Space charge behavior in XLPE cable insulation under 0.2-1.2 MV/cm dc fields," *IEEE Transactions on Dielectrics and Electrical Insulation*, vol. 5, pp. 82-90, 1998.

[26] H. Hussaini, A. A. Adam, and A. A. Susan, "Review of space-charge measurement using Pulsed Electro-Acoustic Method: Advantages and Limitations," *J. Eng. Research Applications*, vol. 5, pp. 90-95, 2015.

[27] G. Rizzo, P. Romano, A. Imburgia, and G. Ala, "Review of the PEA method for space charge measurements on HVDC cables and mini-cables," *Energies*, vol. 12, p. 3512, 2019.

Z. Gibson and J. R. Dennison, "Relevancy of Pulsed Electroacoustic Measurements for Investigating Spacecraft Charging," in IEEE Transactions on Plasma Science, doi: 10.1109/TPS.2023.3244058.

[28] Y. Imaizumi, K. Suzuki, Y. Tanaka, and T. Takeda, "Three-dimensional space charge distribution measurement in solid dielectrics using pulsed electroacoustic method," in *Proceedings of 1995 International Symposium on Electrical Insulating Materials*, 1995, pp. 315-318.

[29] Y. Tanabe, M. Fukuma, A. Minoda, and M. Nagao, "Multi-sensor space charge measurement system on PEA method," *Proceedings lEE Jpn. CFM*, vol. 3, pp. 7-14, 2003.

[30] T. Maeno, "Three-dimensional PEA charge measurement system," *IEEE Transactions on Dielectrics and Electrical Insulation*, vol. 8, pp. 845-848, 2001.

[31] D. Hastings and H. Garrett, *Spacecraft-environment interactions*: Cambridge University Press, 2004.

[32] J. R. Dennison, R. C. Hoffman, and J. Abbott, "Triggering Threshold Spacecraft Charging with Changes in Electron Emission from Materials," presented at the Proceedings of the 45th American Institute of Aeronatics and Astronautics Meeting on Aerospace Sciences, Reno, NV, 2007.

[33] J. R. Dennison, K. Hartley, L. Montierth Phillipps, J. Dekany, J. S. Dyer, and R. H. Johnson, "Small Satellite Space Environments Effects Test Facility," in *28th Annual AIAA/USU Conference on Small Satellites*, Logan, UT, 2014.

[34] R. C. Olsen, "A threshold effect for spacecraft charging," *Journal of Geophysical Research: Space Physics*, vol. 88, pp. 493-499, 1983.

[35] H. B. Garrett, "The charging of spacecraft surfaces," *Reviews of Geophysics*, vol. 19, pp. 577-616, 1981.

[36] H. Garrett, D. Schwank, P. Higbie, and D. Baker, "Comparison between the 30-to 80-keV electron channels on ATS 6 and 1976-059A during conjunction and application to spacecraft charging prediction," *Journal of Geophysical Research: Space Physics*, vol. 85, pp. 1155-1162, 1980.

[37] J. Reagan, R. Nightingale, E. Gaines, R. Meyerott, and W. Imhof, "Role of energetic particles in charging/discharging of spacecraft dielectrics," *NASA. Lewis Research Center Spacecraft Charging Technol., 1980*, 1981.

[38] M. Gussenhoven and E. Mullen, "A'worst case'spacecraft charging environment as observed by SCATHAon 24 April 1979," in *20th Aerospace Sciences Meeting*, 1982, p. 271.

[39] G. Wilson, "The Internal Charge Evolution of Multilayered Materials Undergoing Mono-Energetic Electron Bombardment," PhD, Physics, Utah State University, 2021.

[40] M. J. Berger, J. S. Coursey, M. A. Zucker, and J. Chang. (2005, April 25). *ESTAR, PSTAR, and ASTAR: Computer Programs for Calculating Stopping-Power and Range Tables for Electrons, Protons, and Helium Ions (version 1.2.3) (1.2.3 ed.)*. Available: http://physics.nist.gov/Star

[41] G. Wilson and J. R. Dennison, "Approximation of Range in Materials as a Function of Incident Electron Energy," *IEEE Transactions on Plasma Science*, vol. 40, pp. 291-297, 2012.

[42] G. Wilson, J. R. Dennison, A. E. Jensen, and J. Dekany, "Electron energy-dependent charging effects of multilayered dielectric materials," *IEEE Transactions on Plasma Science*, vol. 41, pp. 3536-3544, 2013.

[43] G. Wilson, A. Starley, L. Phillips, and J. R. Dennison, "A Predictive Range Expression: Applications and Limitations," *IEEE Transactions on Plasma Science*, vol. Pre-print, 2018.

[44] A. V. P. F. Technology, "APTIV 1000 Series Films for Electrical Insulation," https://www.victrex.com/en/datasheets

[45] Z. Gibson and J. R. Dennison, "Uncertainties of the Pulsed Electroacoustic Method: Peak Positions of Embedded Charge Distributions," in *International Conference on Dielectrics*, Palermo, Italy, 2022.

[46] A. Mackova, P. Malinsky, R. Miksova, V. Hnatowicz, R. Khaibullin, P. Slepicka, *et al.*, "Characterisation of PEEK, PET and PI implanted with 80 keV Fe+ ions to high fluencies," *Nuclear Instruments and Methods in Physics Research Section B: Beam Interactions with Materials and Atoms*, vol. 331, pp. 176-181, 2014.

[47] D. Drouin, A. R. Couture, D. Joly, X. Tastet, V. Aimez, and R. Gauvin, "CASINO V2. 42—a fast and easy-to-use modeling tool for scanning electron microscopy and microanalysis users," *Scanning: The Journal of Scanning Microscopies*, vol. 29, pp. 92-101, 2007.

[48] G. Chen, Y. Chong, and M. Fu, "Calibration of the pulsed electroacoustic technique in the presence of trapped charge," *Measurement Science and Technology*, vol. 17, p. 1974, 2006.

[49] L. Galloy, L. Berquez, F. Baudoin, and D. Payan, "High-resolution pulsed electro-acoustic (HR PEA) measurement of space charge in outer space dielectric materials," *IEEE Transactions on Dielectrics and Electrical Insulation*, vol. 23, pp. 3151-3155, 2016.

[50] "Calibration of space charge measuring equipment based on the pulsed electro-acoustic (PEA) measurement principle," International Electrotechnical Commission, IEC TS 62758:2012, 2012.

[51] K. Kumaoka, T. Kato, H. Miyake, and Y. Tanaka, "Development of space charge measurement system with high positionalal resolution using pulsed electro acoustic method," in *Electrical Insulating Materials (ISEIM), Proceedings of 2014 International Symposium on*, 2014, pp. 389-392.

[52] K. Kumaoka, A. Ozaki, H. Miyake, and Y. Tanaka, "Observation of space charge distribution in thin insulating films using improved PEA system," in *Properties and Applications of Dielectric Materials (ICPADM), 2015 IEEE 11th International Conference on the*, 2015, pp. 128-131.

[53] M. Arnaout, K. Chahine, T. Paulmier, and D. Payan, "Model-based processing for the estimation of space-charge distribution from non-contact pulsed electro-acoustic measurements," *Journal of Electrostatics*, vol. 114, p. 103636, 2021/11/01/ 2021.

[54] M. Arnaout, T. Paulmier, B. Dirassen, and D. Payan, "Non-contact in-situ pulsed electro acoustic method for the analysis of charge transport in irradiated space-used polymers," *Journal of Electrostatics*, vol. 77, pp. 123-129, 2015.

[55] Z. Gibson and J. R. Dennison, "A Simple Method for Measuring Shallow Charge Distributions in Dielectrics via Pulsed Electroacoustic Measurements," *IOP Conference Series: Materials Science and Engineering*, To be published.

Zachary Gibson (GS'16) received a B.S. in physics from Utah Valley University in Orem, UT, USA in 2016. He is currently pursuing a PhD in physics at Utah State University in Logan, UT, USA. His research interests include investigation electrical properties of thin film dielectrics, particularly with applications to spacecraft charging, as well as instrumentation of the pulsed electroacoustic method. He has had a Chateaubriand Graduate Fellowship for studies at Université Paul Sabatier in Toulouse, France in 2022 and was a Summer Scholar in the Air Force Research Lab in 2020. IEEE member.

JR Dennison (M'12) received the B.S. degree in physics from Appalachian State University, Boone, NC, in 1980, and the M.S. and Ph.D. degrees in physics from Virginia Tech, Blacksburg, in 1983 and 1985, respectively. He was a Research Associate with the University of Missouri—Columbia before moving to Utah State University (USU), Logan, in 1988. He is currently a Professor of physics at USU, where he leads the Materials Physics Group. He has worked in the area of electron scattering for his entire career and has focused on the electron emission and conductivity of materials related to spacecraft charging for the last three decades. IEEE member.

Z. Gibson and J. R. Dennison, "Relevancy of Pulsed Electroacoustic Measurements for Investigating Spacecraft Charging," in IEEE Transactions on Plasma Science, doi: 10.1109/TPS.2023.3244058.